arXiv:1512.00757v1 [cs.DB] 2 Dec 2015

Tempo: Robust and Self-Tuning Resource Management in Multi-tenant Parallel Databases

Zilong Tan
Duke University
ztan@cs.duke.edu

Shivnath Babu
Duke University
shivnath@cs.duke.edu

Abstract

Multi-tenant database systems have a component called the *Resource Manager, or RM* that is responsible for allocating resources to tenants. RMs today do not provide direct support for performance objectives such as: "Average job response time of tenant A must be less than two minutes", or "No more than 5% of tenant B's jobs can miss the deadline of 1 hour." Thus, DBAs have to tinker with the RM's low-level configuration settings to meet such objectives. We propose a framework called *Tempo* that brings *simplicity*, *self-tuning*, and *robustness* to existing RMs. Tempo provides a simple interface for DBAs to specify performance objectives declaratively, and optimizes the RM configuration settings to meet these objectives. Tempo has a solid theoretical foundation which gives key robustness guarantees. We report experiments done on Tempo using production traces of data-processing workloads from companies such as Facebook and Cloudera. These experiments demonstrate significant improvements in meeting desired performance objectives over RM configuration settings specified by human experts.

1 Introduction

Many enterprises today run multi-tenant database systems on large shared-nothing clusters. Examples of such systems include parallel SQL database systems like RedShift [1], Teradata [5], and Vertica [6], Hadoop/YARN running SQL and MapReduce workloads, Spark running on Mesos [26] or YARN [44], and many others. Meeting the performance goals of business-critical workloads (popularly called *service-level objectives*, or *SLOs*) while achieving high resource utilization in multi-tenant database systems has become more important and challenging than ever.

The problem of handling many (often in 1000s) small and independent databases on a multi-tenant database Platform-as-a-Service (usually called *PaaS* or *DBaaS*) has received considerable attention in recent years [48, 37, 32, 36, 16]. That is not the problem we focus on in this paper. Our focus is on handling fewer, but much "bigger", tenants who process very large amounts of data on a shared-nothing cluster that is usually run within an enterprise. Hadoop, Spark, Teradata, Vertica, etc., are typically run in such settings.

These multi-tenant database systems each have a component—commonly referred to as the *Resource Manager (RM)* (also sometimes called *Workload Manager*)—that is responsible for allocating resources to tenants. Most widely deployed RMs like YARN and Mesos do not support SLOs. Instead, they rely on the Database Administrator (DBA) to "guesstimate" answers to questions such as: "How much resources are needed to complete this job before its deadline?" Then, DBAs have to translate their answers into low-level configuration settings in the RM. This process is brittle and increasingly hard as workloads evolve, data and cluster sizes change, and new workloads are added. Thus, techniques have been proposed in the literature to support specific SLOs such as deadlines [14, 33, 20, 45], fast job response times [10, 14, 23, 39], high resource utilization [2, 10, 14], scalability [2, 41, 49], and transparent failure recovery [49].

In this paper, we present a framework called *Tempo* that brings three properties to existing RMs: *simplicity*, *self-tuning*, and *robustness*. First, Tempo provides a simple interface for DBAs to specify SLOs declaratively. Thus, Tempo enables the RM to be made aware of SLOs such as: "Average job response time of tenant A must be less than two minutes", and "No more than 5% of tenant B's jobs can miss the deadline of 1 hour." Second, Tempo constantly monitors the SLO compliance in the database, and adaptively optimizes the RM configuration settings to maximize SLO compliance. Third, Tempo has a solid theoretical foundation which gives five critical robustness guarantees:

1) Tempo's optimization and modeling algorithms account for the noisy nature of production database systems.
2) Tempo's optimization algorithm converges provably to a Pareto-optimal RM configuration given that satisfying multiple tenant SLOs is a multi-objective optimization problem.
3) When all SLOs cannot be satisfied—which is common

in busy database systems—Tempo guarantees max-min fairness over SLO satisfactions [34].
4) Tempo adapts to workload patterns and variations.
5) Tempo reduces the risk of major performance regression while being applied to production database systems.

We have implemented Tempo as a drop-in component in the RMs used by multi-tenant databases running on Hadoop and Spark. We report experiments done using production traces of data-processing workloads from companies such as Facebook and Cloudera. These experiments demonstrate significant improvements in meeting the SLOs over the original RMs used in five real-life scenarios. For example, Tempo can reduce the average job response time by 50% for best-effort workloads and increase resource utilization by 15%, without hurting the deadline-driven workloads.

2 Production System Experiences

Tempo's design was motivated by our observations from several large production database systems. While designing Tempo, we analyzed workload traces from three companies each of which runs multi-tenant database systems on large clusters. Two of these systems run on 600+ nodes while the other runs on about 150 nodes. (While all three are well-known companies, we cannot share their names due to legal restrictions.) We talked to business analysts, application developers, team managers, and DBAs in these teams to understand the SLOs that they need to meet and the challenges they face in resource management. From all our interviews, the following emerged as the top concerns:

- Concern A: Deadline-based workloads and best-effort workloads have to be supported on the same database system.
- Concern B: Repeatedly-run jobs often have unpredictable completion times.
- Concern C: Resource utilization was lower than expected.
- Concern D: Resource allocation does not adapt automatically to the patterns and variations in the workloads.

To elaborate on these four concerns, we will use one of the three companies—henceforth, referred to as Company ABC—which is a real-life company that runs a multi-tenant database system on a 700-node Hadoop cluster with over 30 Petabytes of data.

2.1 Concern A

Company ABC has three types of users who generate database workloads. Business Intelligence (BI) analysts and Data Scientists predominantly do exploratory analysis on the data. Engineers develop and maintain recurring jobs that run on the database. One such category of jobs is Extract-Transform-Load (ETL) which brings new data into the system. Each job goes through many runs in a development phase on the cluster before being certified to run as a production job. Thus, the system supports both development and production runs of jobs.

Tenant	Characteristics
BI	I/O-intensive SQL queries
DEV	Mixture of different types of jobs
APP	Small, lightweight jobs
STR	Hadoop streaming jobs
MV	Long-running, CPU-intensive
ETL	I/O-intensive, periodic but bursty

Table 1: Tenant characteristics at Company ABC.

Distinct workloads from these users form the *tenants* in the multi-tenant system. Table 2.1 shows the six tenants at Company ABC and their distinct workload characteristics. (The experimental evaluation section gives more fine-grained details of these workloads.)

The BI and ETL users correspond directly to similarly-named tenants. Among the other tenants, MV corresponds to the creation of *Materialized Views* such as joined results of multiple tables as well as statistical models created from the incoming data brought through ETL. The BI users and Data Scientists usually write their queries and analysis programs on these materialized views. The APP tenant runs jobs from a specific high-priority production application. The DEV and STR tenants mostly comprise queries and analysis programs being run as part of application development by engineers and Data Scientists. At Company ABC:

- Jobs from the ETL and MV tenants have deadlines because any delay in these jobs will affect the entire daily operations of the company. We have seen multi-day delays caused by deadline misses for the ETL and MV tenants that had significant business impact.
- About 30% of high-priority jobs in APP miss deadlines.
- While all tenants want as low job response time as possible for completion of their jobs, BI, DEV, and STR are treated as "best-effort" tenants in that the goal is to provide their jobs as low response time as possible subject to meeting the requirements of the ETL, MV, and APP tenants.

2.2 Concern B

Predictability of completion time for recurring jobs is a key need in most companies. This demand stems from ease of resource planning and scheduling for dependent jobs. At Company ABC:

- The completion of one of the recurring jobs of the ETL tenant varies between 5 and 60 minutes.
- The completion of one of the recurring jobs of the MV tenant varies between 2 and 6 hours.

While we observed that this variance is caused partly by variation in the input sizes of the jobs across runs, these sizes exhibit strong temporal patterns. For example, the input sizes

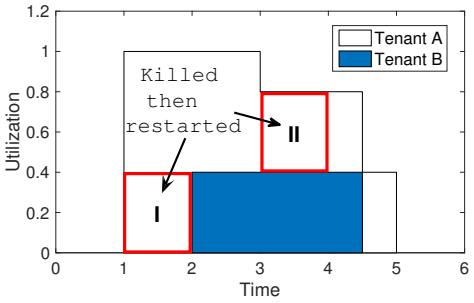

Figure 1: Wasted utilization due to preemption.

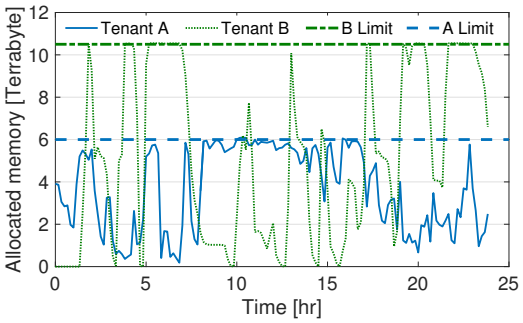

Figure 2: Memory consumption of two tenants during a day.

of the recurring jobs in ETL vary across days within a week, but remain stable across multiple weeks.

2.3 Concern C

Resources can be wasted in multi-tenant systems due to reasons such as: (i) task preemption; (ii) suboptimal configuration of resource limits; and (iii) jobs in poorly-written queries being killed by DBAs. Figure 1 illustrates the impact of preemption based on two tenants, A and B. Tenant A first launched some tasks and used up all the resources, yielding 100% resource utilization. Suppose B submitted tasks just after the resources were grabbed by A. Then, without preemption, B's tasks will have to wait until A's tasks finish; which could cause B to miss its deadlines.

On the other hand, suppose a preemption timeout of 1 time unit is configured for B. Then, preemptions will take place at time 2 killing the most recently launched tasks of Tenant A, and B will acquire the freed resources immediately after. However, A's tasks will lose the unfinished work and then be restarted at time 3. The region marked I in Figure 1 corresponds to the resources taken by the killed tasks of A that were preempted. This figure shows that even if the resource utilization between time 1 and time 3 remained 1.0 (100%), the *effective utilization*, which excludes region I, is only 80%.

At Company ABC, 17.5% of map tasks and 27.7% of reduce tasks were preempted for the jobs run by the MV tenant over a week interval. This caused considerable amount of wasted resources, especially because the reduce tasks of the MV tenant have long execution times.

2.4 Concern D

A resource allocation which meets the SLOs perfectly at one moment may not be suboptimal at another moment due to various factors. First, input data sizes for a tenant may vary considerably across shorter time intervals while showing distinct patterns across longer intervals. At Company ABC, ETL jobs process Web activity logs which come in much smaller quantities on weekends.

Second, the resource demands of different tenants can be correlated over time. For example, Figure 2 shows the memory consumption of two tenants at Company ABC over the course of a day. The horizontal lines in the figure show the respective resource limits that have been configured by the DBA to protect against resource hoarding by tenants. Notice that while there are periods where both tenants use up all available resources, there are other periods where the configured resource limit prevents one tenant from using the resources unused by the other.

3 Overview of Problem

From our interviews, two salient points emerged that summarize the crux of what Tempo attempts to solve:

- Workloads in multi-tenant parallel databases have SLOs. Current RMs do not provide easy ways to ensure that these SLOs are satisfied.
- Current RMs require the DBA to estimate resources to meet the per-tenant SLOs, and then specify low-level RM configuration like resource shares, resource limits, and preemption timeouts in order to meet these SLOs. This process is brittle and increasingly hard as workloads evolve, data and cluster sizes change, and new workloads are added.

3.1 SLOs

From our interviews with users and DBAs, we identified five major classes of SLOs. The first class specifies job deadlines. For recurring jobs, the deadline is either the start of the next run or an absolute time point like 5:00 AM. The second class specifies that job response time must be less than a given threshold. Such SLOs are often associated with ad-hoc jobs. The third class is about ensuring that each tenant gets a fair allocation of resources. In particular, when the database is under contention, the proportion of resources allocated to each tenant must adhere to predetermined values. This SLO class prevents individual tenants from monopolizing the resources intentionally or otherwise. Fourth, the resource utilization or job throughput must be above a threshold. This SLO class generally serves the interest of DBAs to maximize the return on investment (ROI) in the cluster. A fifth type of SLO orders the other SLOs in terms of priority. This special SLO

mandates that SLOs with higher priorities be considered first when not all SLOs can be met with the resources available.

3.2 RM Configuration Space

In this section, we will describe the typical set of configuration parameters supported by modern RMs on a per-tenant basis. As we will describe in later sections, Tempo adaptively computes the settings for these per-tenant RM configuration parameters in order to maximize SLO compliance.

Parallel databases decompose queries and analysis programs to DAGs (Directed Acyclic Graphs) of jobs that each consist of one or more parallel tasks. CPU, Memory, and other resources are allocated to these tasks. The resources allocated to any tenant can be captured in a fine-grained manner based on the start time, end time, and the resource allocation vector d for each of the tasks run on behalf of the tenant.

In this paper, for ease of exposition, we will consider a uni-dimensional representation of d as an integer number of *containers* (or *slots*) as done in RMs like Mesos and YARN. Namely, a task is run in a container that is allocated on behalf of a tenant who submits the task. No two tasks can share the same container. The RM of a multi-tenant database system has a fixed total number of containers that it can allocate across all tenants at any point of time. This allocation is governed by a set of configuration parameters for each tenant. These parameters fall into three categories, described next.

Resource Shares: The resource share for a tenant specifies the proportion of total resources that this tenant should get with respect to other tenants. For example, suppose there are three tenants A, B, and C with shares in the ratio 1:2:3 respectively. Suppose the database system has 12 containers that it can allocate at any point of time. Then, if all tenants have tasks to run, then tenants A, B, and C will get 2, 4, and 6 containers respectively.

Suppose a tenant does not have tasks to run in its full quota of resources. Then, the unused quota of resources will be allocated to other tenants who have tasks to run. This allocation will be proportional to the resource shares of the other tenants. In the example above, suppose tenant C has no tasks to run, but A and B have many tasks to run. Then, tenants A and B will get 4 and 8 containers respectively.

Resource Limits: For any tenant, minimum and maximum limits can be specified for the resources that this tenant can get at any point of time. In the example above where tenants A, B, and C have shares in the ratio 1:2:3 respectively, suppose all tenants have many tasks to run, but the maximum resource limit for tenant C is set to 3. Then, tenants A, B, and C will get 3, 6, and 3 containers respectively. Limits are often specified to ensure two things: (i) no tenant can monopolise all resources, and (ii) critical workloads from a tenant can start running as quickly as possible.

Resource Preemption: For any tenant, a configuration can be set to preempt—after a certain time interval that the tenant should wait for—tasks from other tenants that using resources that are rightly owed to this tenant. Such preemption will free up resources for this tenant. There are two levels of preemption timeouts. One level of preemption is when the tenant's current resource allocation is below its configured resource share. The other, and more critical level, is when the tenant's current resource allocation is below its configured minimum resource limit.

Preemption is important in multi-tenant systems. Without preemption, a low-priority tenant who submitted tasks earlier than a high-priority tenant can cause the high-priority tenant to miss deadlines. Preemption can be implemented by suspending tasks or by killing tasks running in the container. While task suspension is the preferred mechanism, it is not supported in most multi-tenant systems that are commonly used today. As we showed in Section 2.3, if the two levels of preemption timeouts are not configured carefully, then preemption by killing tasks can cause a lot of wasted work and low resource utilization.

3.3 Role of Tempo

Our interviews revealed that DBAs manually tune the per-tenant RM configuration parameters in order to meet tenant SLOs. For example, at Company ABC, the RM configuration is tuned whenever tenants complain about deadline or job response time SLOs not being met. This process is brittle because it is hard for the DBAs to take into account the workload patterns and evolution, constant addition of new workloads, and the multiple objectives and tradeoffs. The goal of Tempo is to make this process easy and principled.

4 Tempo

As discussed in Section 1, Tempo is designed to bring three properties to existing RMs: simplicity, self-tuning, and robustness. As part of simplicity, Tempo introduces the concept of *QS (Quantitative SLO)*. A QS is a quantitative metric defined per SLO to measure the satisfaction of the SLO at any point of time. In Section 5, we will show how the QS concept supports several tenant SLOs that arise in real-life use cases.

Operationally, the QS for an SLO can be thought of in two ways (recall Section 3.2):

1. As a function $f(\boldsymbol{x}; w)$ where w denotes the workload and $\boldsymbol{x}$ is the vector representation of the parameters in the RM configuration used to allocate resources to process w.
2. As a function of the actual task resource allocation schedule (henceforth called *task schedule*) that is produced when the workload w runs under $\boldsymbol{x}$.

As we will show in Section 5, it is conceptually easier for humans to understand and use the QS concept when defined in terms of the task schedule. At the same time, Tempo needs the $f(\boldsymbol{x}; w)$ notion in order to create a modular architecture

that provides self-tuning and robustness. Figure 3 shows how this modular architecture drives the repeated execution of Tempo's control loop.

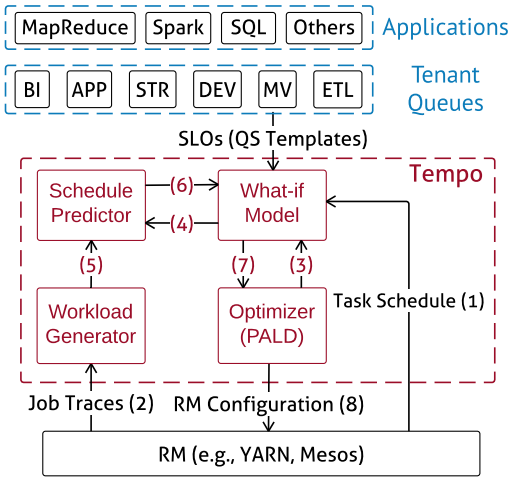

Figure 3: Tempo architecture: tenants specify SLOs using the QS templates, and Steps (1)-(8) form the Tempo control loop.

The Tempo control loop consists of the eight steps denoted (1)-(8) in Figure 3. The inputs to the Tempo control loop are the SLOs defined for each tenant (which can be specified conveniently via predefined templates as discussed in Section 5). Step (1) of the control loop extracts the recent task schedule for evaluating QS metrics for the input SLOs under the current RM configuration $\boldsymbol{x}$. Through Steps (2)-(8), Tempo replaces the current RM configuration $\boldsymbol{x}$ with a new one $\boldsymbol{x'}$; concluding one iteration of the control loop. Once the QS metrics for the input SLOs under $\boldsymbol{x'}$ are observed at Step (1) of the next iteration, the Tempo control loop will revert the RM configuration $\boldsymbol{x'}$ back to $\boldsymbol{x}$ if the currently observed QS metrics do not dominate the previously observed ones. This mechanism adds robustness in Tempo by guarding against performance degradation during the self-tuning approach.

Steps (2)-(8) are orchestrated by Tempo's *Optimizer* which applies a self-tuning algorithm called *PALD*. PALD is a novel multi-objective optimization algorithm that we developed for the noisy environments seen in production multi-tenant parallel database systems. As we will show in Section 6, PALD *provably* converges to a RM configuration that provides a Pareto-optimal setting for the QS metrics of the input SLOs. In addition, whenever available resources are insufficient to fully satisfy all SLOs, PALD handles the SLO tradeoffs gracefully by minimizing the largest regret across all SLO satisfactions as measured by the QS metrics.

In Steps (2)-(8), the Optimizer explores a set of RM configurations by proposing the RM configurations (3)-(4), getting the simulated task schedule (6) of the workloads (5) based on the job traces (2). The predicted QS metrics under these RM configurations are passed back to the Optimizer (7) to compute a Pareto-improving RM configuration (8). To implement these steps, the Optimizer uses three other components as shown in Figure 3: *Workload Generator*, *Schedule Predictor*, and *What-if Model*.

The Workload Generator replays historical job traces or synthesizes workloads with given characteristics. The Schedule Predictor produces the simulated task schedule of the generated workloads under given RM configurations. The What-if Model evaluates the QS metrics for the input SLOs using the simulated task schedule. Together, the three components enable the Optimizer to explore the impact of different RM configurations on the input SLOs and use the PALD algorithm (described in Section 6) to produce Pareto-optimal RM configurations for these SLOs.

While proposing RM configurations in Step (3), the Optimizer meticulously generates configurations only within a given maximum distance to the currently used RM configuration. Tempo uses normalized l^2-norm as the distance metric, and allows the DBA to specify the maximum distance based on her risk tolerance. This technique further reduces the risk of causing dramatic impact on the running workloads when applying a new RM configuration; which is particularly desirable in production environments.

5 QS: Quantifiable Metrics to Measure SLO Satisfaction

A key design goal in Tempo was to provide a quantitative understanding of how the workload and RM configuration impact each SLO. We developed the QS metric which can be used to compare the relative SLO satisfactions under different workloads and RM configurations. Minimizing the QS metric improves the corresponding SLO. QS metrics were motivated by the idea of loss functions in machine learning.

The QS metric for an SLO is defined as a function of the resulting task schedule for a workload under a given RM configuration. Recall from Section 3.2 that a task schedule consists of start time, end time, and the resource allocation d for each of the tasks run on behalf of a tenant. For ease of exposition, d can be considered as an integer number of containers as done in RMs like Mesos and YARN.

5.1 QS Metrics for Popular SLOs

We will now describe QS metrics for the common classes of SLOs that we came across in our interview (recall Section 3.1). Note that SLOs and corresponding QS metrics can be defined at different levels such as at the level of a recurring job, at the level of the entire workload of a tenant, at the level of the entire cluster, etc. In this section, we will define QS metrics at the job level, but the ideas generalize. Consider a certain interval of time L. Let J_i denote the set of jobs from tenant i which was submitted and completed during this interval. Let T_i be the set of tasks associated with J_i. Based on

this notation, we can define the following QS metrics for the common SLOs.

Low average job response time: The QS metric for job response time SLO takes the average across all jobs executed by the tenant, as given by (1) where t_j^s and t_j^f are the submission and finish time of job j, respectively. $|J_i|$ represents the cardinality of the job set J_i.

$$\mathrm{QS}_{\mathrm{AJR}}(J_i) = \frac{1}{|J_i|} \sum_{j \in J_i} \left(t_j^f - t_j^s \right). \tag{1}$$

Deadlines: The QS metric for deadline SLO can be defined as the fraction of jobs of a tenant that missed their deadline. Let t_j^d be the deadline of the job j, the deadline QS metric can be defined as

$$\mathrm{QS}_{\mathrm{DL}}(J_i) = \frac{1}{|J_i|} \sum_{j \in J_i} \mathbb{I}\left(t_j^f > \gamma \left(t_j^f - t_j^l \right) + t_j^d \right), \tag{2}$$

where $\mathbb{I}(\cdot)$ is the indicator function, and γ is a slack (tolerance) when identifying the deadline violation. That is, a job j is considered violating the deadline t_j^d only if its completion is later than the deadline by a factor γ in terms of the job duration $t_j^f - t_j^l$. The slack makes the QS metric less sensitive to system variability.

High resource utilization: The resource utilization can be calculated as the integral of the fraction of overall resources allocated to the tenant over the time interval. This utilization amounts to the area of the shaded region in Figure 4. We can use the *dominant resource usage* when multiple resource types are considered [22, 21, 42]. Note that the dominant resource usage is represented by a ratio between zero and one. When there is only a single resource type, we normalize the resource usage. Recall that the optimization minimizes the

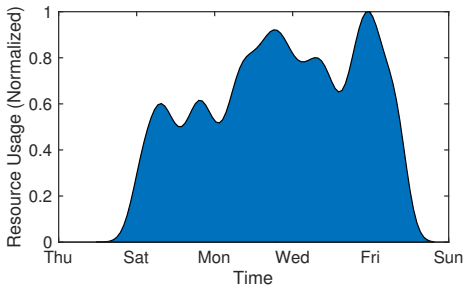

Figure 4: Normalized (dominant) resource usage over a period of time. The shaded area corresponds to the resources allocated to a particular tenant.

QS metrics. Thus, we can define the QS metric for achieving high resource utilization as the negative area in Figure 4, which is given by

$$\mathrm{QS}_{\mathrm{UTIL}}(J_i) = -\frac{1}{L} \sum_{j \in T_i} d_j \left(t_i^f - t_t^l \right), \tag{3}$$

where L be the length of the interval, and d_j is the amount of resources allocated to task j. This QS metric can also be applied to evaluate the impact of preemption, as illustrated in Figure 1, by comparing the QS values computed using all tasks versus using only tasks that were not preempted.

High job throughput: The job throughput is defined as the number of jobs submitted and completed within the interval. The QS metric for achieving high job throughput is thus given by

$$\mathrm{QS}_{\mathrm{THR}}(J_i) = -|J_i|. \tag{4}$$

Resource fairness: The fairness can be defined by comparing the relative ratio of resource utilization used by the tenants versus the desired ratio. This definition is also known as the long-term fairness [43]. Let c_i denote the desired share of resources, the fairness QS metric follows

$$\mathrm{QS}_{\mathrm{FAIR}}(J_i) = -\left| c_i + \mathrm{QS}_{\mathrm{UTIL}}(J_i) \right|.$$

5.2 QS Templates

To further simplify the use of Tempo, we implemented *QS templates* to enable tenants to specify SLOs declaratively. A QS template specifies: (a) a unique queue to which the tenant submits its workload, (b) a predefined QS metric definition (e.g., the ones given above), (c) one or more optional parameters associated with the corresponding SLO (e.g., the value of a deadline, or a threshold on job response time), and (d) an optional priority value (priorities are incorporated by multiplying the QS metric with the priority value). Tempo's QS templates make it easy to make the RM aware of SLOs such as: "Average job response time of tenant A must be less than two minutes", and "No more than 5% of tenant B's jobs can miss the deadline of 1 hour."

6 Tempo's Theoretical Foundations

6.1 Multi-objective QS Optimization Problem

Tempo's Optimizer is given SLOs by the tenants and solves the following problem:

$$\begin{array}{lll} \text{minimize} & \mathbb{E}\left[\left(f_1(\boldsymbol{x}; w), \cdots, f_k(\boldsymbol{x}; w) \right) \right] & \text{(SP1)} \\ \text{subject to} & \mathbb{E}\left[f_i(\boldsymbol{x}; w) \right] \leq r_i & \forall i = 1, 2, \cdots, k. \\ & \boldsymbol{x} \in \mathscr{X}. & \end{array}$$

Here, $f_1(\boldsymbol{x}; w), f_2(\boldsymbol{x}; w), \cdots, f_k(\boldsymbol{x}; w)$ denote QS functions for the k SLOs from tenants, under workload w and RM configuration $\boldsymbol{x}$. Since measurements of the QS metrics will be noisy in a production database system, the expectation $\mathbb{E}(\cdot)$ in (SP1) is to average out the impact of noise. The vector minimization in (SP1) is in Pareto optimal sense: an RM configuration $\boldsymbol{x}$ is said to dominate another configuration $\boldsymbol{x'}$, if for all

$i \in [k]$, $f_i(\boldsymbol{x};w) \leq f_i(\boldsymbol{x}\prime;w)$, with at least one inequality. An RM configuration is called weak Pareto-optimal if no other RM configuration dominates it. $\mathscr{X}$ is the RM configuration space defined in Section 3.2. The r_i values are used to specify constraints that are part of SLOs. Tempo converts all SLOs into such constraints so that a solution to (SP1) will enforce all SLOs. In order to keep improving on the current RM configuration as part of self-tuning, Tempo's control loop can use the QS value attained for an SLO at the current configuration as the r_i for the next iteration.

As an example, let us consider two tenants A and B. A has a deadline SLO while B is a best-effort tenant that cares about getting the least possible job response times. For Tempo's Optimizer, A's deadline SLO will become a constraint $\mathbb{E}[f_1(\boldsymbol{x};w)] \leq r_1$, where r_1 is A's tolerable fraction of deadline violations and f_1 is the QS function for deadline SLO from Section 5.1. B's SLO for getting the lowest possible job response time can be expressed as a constraint $\mathbb{E}[f_2(\boldsymbol{x};w)] \leq r_2$, where f_2 is the QS function for response time SLO from Section 5.1 and r_2 is the average job response time for B's jobs obtained with the current RM configuration.

One can also prioritize certain SLOs over others in (SP1) by weighting the corresponding QS functions. For instance, to promote the priority of an SLO whose QS is $f_i(\boldsymbol{x};w)$, we can replace the QS with $\alpha f_i(\boldsymbol{x};w)$, where $\alpha > 1$ is the magnitude of the promotion.

6.2 Goals and Notation

We now present a novel *PAreto Local Descent (PALD)* algorithm for solving the multi-objective QS optimization problem (SP1). QS optimization poses two challenges which are not fully addressed by existing methods: 1) the QS measurements are noisy due to inaccuracies in job traces, choice of time intervals, etc.; and 2) QS metrics are expensive to estimate as each prediction of a QS metric involves a task scheduling simulation. Existing approaches roughly fall into three classes. The first class uses evolutionary algorithms [17, 18, 31], which are sensitive to noise and require extensive QS predictions. The second class is prediction-based [50], which inherently does not guarantee an optimal solution. A third class achieves objectives which are different from Pareto-optimality [35, 29]. In the following sections, we describe PALD, and prove that it can handle the two challenges.

We denote vectors and matrices by boldface symbols. The simplified notations f_i and $f_i(\boldsymbol{x})$ are used interchangeably to refer to the QS metric function $f_i(\boldsymbol{x};w)$, and we use $\boldsymbol{f}(\boldsymbol{x})$ to refer to the vector of QS functions. For each QS metric, we denote the average of N measures by $f_i(\boldsymbol{x})$.

The goal of PALD is to find a weak Pareto-optimal solution to (SP1). If a feasible solution exists, then the resulting RM configuration satisfies the "hard" SLOs represented by the constraints in (SP1), while improving the "best-effort" SLOs. If there is no feasible solution, then the resulting RM configuration balances the SLOs represented by the constraints based on max-min fairness. This feature supports prioritizing the SLOs by weighting the corresponding constraints.

6.3 Proxy Model

The key technique used in PALD is a proxy model, which transforms the original problem (SP1) to a proxy problem (SP2) such that all solutions to the proxy problem are solutions to the original one, but not the other way around. We show that the proxy problem can be solved efficiently.

First, it should be noted that the well-known *weighted sum scalarization* ([11])—which converts the multi-dimensional QS vector to a scalar by taking a weighted sum of the QS functions—does not apply in this case; for it does not ensure the first set of constraints in the problem (SP1). For example, consider two RM configurations and two QS functions. Suppose that the QS vectors corresponding to the two solutions are $(5,5)^\top$ and $(0,7)^\top$, respectively. Let $\boldsymbol{r} = (6,6)^\top$. When the weights are equal, the optimization using weighted sum scalarization yields the QS vector $(0,7)^\top$, which does not dominate $\boldsymbol{r} = (6,6)^\top$.

Our solution PALD solves the following proxy problem:

$$\begin{aligned} \text{minimize} \quad & \boldsymbol{c}^\top [\boldsymbol{f}(\boldsymbol{x}) - \rho \max(\boldsymbol{f}(\boldsymbol{x}), \boldsymbol{r})] && \text{(SP2)} \\ \text{subject to} \quad & \mathbb{E}[f_i(\boldsymbol{x})] \leq r_i && \forall i = 1,2,\cdots,k. \\ & \boldsymbol{x} \in \mathscr{X}. \end{aligned}$$

Here, $\boldsymbol{c}$, which is a positive vector, and $\rho < 1$ are two parameters whose values will be described in Section 6.3.1. The parameter ρ penalizes those QS functions $f_i(\boldsymbol{x}) > r_i$, and is independent of the vector $\boldsymbol{c}$. This is an advantage over *conic scalarization* [29]. One special case is that when $\rho = 0$, the problem (SP2) becomes the weighted sum scalarization.

Theorem 1. *For any arbitrary positive vector $\boldsymbol{c}$ and parameter $\rho < 1$, every solution of* (SP2) *is a solution for* (SP1).

Proof. Let $s_i(\boldsymbol{x}) = c_i[f_i(\boldsymbol{x}) - \rho \max(f_i(\boldsymbol{x}), r_i)]$, the objective of problem (SP2) can be written as

$$\begin{aligned} \sum_i s_i(\boldsymbol{x}) &= \sum_{i:f_i(\boldsymbol{x}) \leq r_i} s_i(\boldsymbol{x}) + \sum_{j:f_j(\boldsymbol{x}) > r_j} s_j(\boldsymbol{x}) \\ &= \sum_{i:f_i(\boldsymbol{x}) \leq r_i} c_i[f_i(\boldsymbol{x}) - \rho r_i] + && (5) \\ &\quad \sum_{j:f_j(\boldsymbol{x}) > r_j} c_j(1-\rho) f_j(\boldsymbol{x}). && (6) \end{aligned}$$

Both (5) and (6) are strictly monotonically increasing with respect to $f_i(\boldsymbol{x})$, so is the objective (SP2). Consider a solution $\boldsymbol{x}$ for (SP2). Suppose that $\boldsymbol{x}$ is not a weak Pareto-optimal solution for (SP1), then there exists another weak Pareto-optimal solution $\boldsymbol{x}\prime$ for the problem (SP1) that dominates $\boldsymbol{x}$. However, this contradicts the hypothesis that $\boldsymbol{x}$ is a solution for the problem (SP2), due to the monotonicity. □

6.3.1 Parameters

We now derive the parameters $\boldsymbol{c}$ and ρ in the proxy model (SP2). PALD uses the stochastic gradient descent for solving the proxy problem, and the gradients are estimated using the well-known LOESS [13]. Let $s(\boldsymbol{x})$ denote the objective of the proxy problem (SP2), the update for each iteration is given by

$$\boldsymbol{x}^{new} = \boldsymbol{x}^{old} - \alpha \nabla_{\boldsymbol{x}} s(\boldsymbol{x}), \tag{SGD}$$

where α is the step size. The parameters $\boldsymbol{c}$ and ρ are chosen such that the above update does not increase those QS functions $f_i(\boldsymbol{x}) \geq r_i$. We thereby obtain $\forall i : f_i(\boldsymbol{x}) \geq r_i$, $-\alpha \nabla_{\boldsymbol{x}}{}^{\top} f_i(\boldsymbol{x}) \nabla_{\boldsymbol{x}} s(\boldsymbol{x}) \leq 0$, or equivalently $\nabla_{\boldsymbol{x}}{}^{\top} f_i(\boldsymbol{x}) \nabla_{\boldsymbol{x}} s(\boldsymbol{x}) \geq 0$. The parameters are also chosen to best improve those violated constraints $f_i(\boldsymbol{x}) \geq r_i$. Fixing $\boldsymbol{c}, \rho$ is obtained by solving

$$\begin{aligned} &\arg\max_{\rho} \min_{i:f_i(\boldsymbol{x})\geq r_i} \nabla_{\boldsymbol{x}}{}^{\top} f_i(\boldsymbol{x}) \nabla_{\boldsymbol{x}} s(\boldsymbol{x}) && \text{(RHO)} \\ \text{s.t.} \quad &\nabla_{\boldsymbol{x}}{}^{\top} f_i \nabla_{\boldsymbol{x}} s(\boldsymbol{x}) \geq 0, \quad \forall i : f_i(\boldsymbol{x}) \geq r_i \\ &\boldsymbol{c} \geq 0, \quad \rho < 1. \end{aligned}$$

Note that the objective of the proxy model (SP2) is not differentiable at points $\{\boldsymbol{x} \in \mathscr{X} : \boldsymbol{f}(\boldsymbol{x}) = \boldsymbol{r}\}$, and we need to condition on the subgradients. Let us first assume that $\partial s(\boldsymbol{x}) / \partial f_j(\boldsymbol{x})\big|_{x=r} = c_j(1-\rho)$. The objective of the problem (RHO) can be rewritten as

$$\sum_j c_j \nabla_{\boldsymbol{x}}{}^{\top} f_i \nabla_{\boldsymbol{x}} f_j - \rho \sum_{j:f_j(\boldsymbol{x})\geq r_j} c_j \nabla_{\boldsymbol{x}}{}^{\top} f_i \nabla_{\boldsymbol{x}} f_j. \tag{7}$$

Based on the range of the subgradient of $s(\boldsymbol{x})$, we can bound ρ. To satisfy the first set of constraints in the problem (RHO) at an indifferentiable point, we have that

$$\min_{i, \frac{\partial s}{\partial f_j} : f_i(\boldsymbol{x})\geq r_i} \sum_j \nabla_{\boldsymbol{x}}{}^{\top} f_i \nabla_{\boldsymbol{x}} f_j \frac{\partial s}{\partial f_j} \geq 0. \tag{8}$$

Now consider separately two cases $\rho \geq 0$ and $\rho < 0$. When $\rho \geq 0$ the inequality (8) is equivalent to $\forall i : \nabla_{\boldsymbol{x}} f_i \neq \boldsymbol{0} \wedge f_i(\boldsymbol{x}) \geq r_i$ that

$$\begin{aligned} (1-\rho) c_i \nabla_{\boldsymbol{x}}{}^{\top} f_i \nabla_{\boldsymbol{x}} f_i &\geq - \sum_{j:j\neq i} \min_{\partial s/\partial f_j} \nabla_{\boldsymbol{x}}{}^{\top} f_i \nabla_{\boldsymbol{x}} f_j \frac{\partial s}{\partial f_j} \\ &= -(1-\rho) \sum_{\substack{j:j\neq i, \\ \nabla_{\boldsymbol{x}}{}^{\top} f_i \nabla_{\boldsymbol{x}} f_j \geq 0}} c_j \nabla_{\boldsymbol{x}}{}^{\top} f_i \nabla_{\boldsymbol{x}} f_j \\ &\quad - \sum_{\substack{j:j\neq i, \\ \nabla_{\boldsymbol{x}}{}^{\top} f_i \nabla_{\boldsymbol{x}} f_j < 0}} c_j \nabla_{\boldsymbol{x}}{}^{\top} f_i \nabla_{\boldsymbol{x}} f_j, \end{aligned}$$

which simplifies to

$$0 \leq \rho \leq \min_{\substack{i:\nabla_{\boldsymbol{x}} f_i \neq \boldsymbol{0}, \\ f_i(\boldsymbol{x})\geq r_i}} \frac{\sum_j c_j \nabla_{\boldsymbol{x}}{}^{\top} f_i \nabla_{\boldsymbol{x}} f_j}{\sum_{j:\nabla_{\boldsymbol{x}}{}^{\top} f_i \nabla_{\boldsymbol{x}} f_j \geq 0} c_j \nabla_{\boldsymbol{x}}{}^{\top} f_i \nabla_{\boldsymbol{x}} f_j}.$$

Similarly, we can obtain the bound for the case $\rho < 0$. It should be noted that these bounds are useful only when the following conditions are satisfied:

$$\sum_j c_j \nabla_{\boldsymbol{x}}{}^{\top} f_i \nabla_{\boldsymbol{x}} f_j \geq 0, \quad \forall i : \nabla_{\boldsymbol{x}} f_j \neq \boldsymbol{0} \wedge f_i(\boldsymbol{x}) \geq r_i. \tag{9}$$

These conditions can be satisfied for convex QS functions, using the vector $\boldsymbol{c}$ described in MGDA [19]. Combining the results arrives at the optimal choice of ρ for the problem (RHO):

$$\rho_* = \begin{cases} \min\limits_{\substack{i:\nabla_{\boldsymbol{x}} f_j \neq \boldsymbol{0}, \\ f_i(\boldsymbol{x})\geq r_i}} \dfrac{\sum_j c_j \nabla_{\boldsymbol{x}}{}^{\top} f_i \nabla_{\boldsymbol{x}} f_j}{\sum_{j:\nabla_{\boldsymbol{x}}{}^{\top} f_i \nabla_{\boldsymbol{x}} f_j \geq 0} c_j \nabla_{\boldsymbol{x}}{}^{\top} f_i \nabla_{\boldsymbol{x}} f_j}, & \rho \geq 0 \\ \max\limits_{\substack{i:\nabla_{\boldsymbol{x}} f_j \neq \boldsymbol{0}, \\ f_i(\boldsymbol{x})\geq r_i}} \dfrac{\sum_j c_j \nabla_{\boldsymbol{x}}{}^{\top} f_i \nabla_{\boldsymbol{x}} f_j}{\sum_{j:\nabla_{\boldsymbol{x}}{}^{\top} f_i \nabla_{\boldsymbol{x}} f_j < 0} c_j \nabla_{\boldsymbol{x}}{}^{\top} f_i \nabla_{\boldsymbol{x}} f_j}, & \rho < 0. \end{cases}$$

The sign of the parameter ρ depends on the last term of the objective (7) as to maximize the objective. To deliver the above optimal ρ_*, the vector $\boldsymbol{c}$ must also satisfy the conditions (9).

To achieve max-min fairness of SLOs, PALD chooses $\boldsymbol{c}$ that improves the most violated constraint, through the following linear program.

$$\begin{aligned} \text{maximize} \quad & z \\ \text{subject to} \quad & \boldsymbol{J}_{i:f_i(\boldsymbol{x})\geq r_i} \boldsymbol{J}^{\top} \boldsymbol{c} \geq z\boldsymbol{1} \\ & \boldsymbol{c} \geq 0, \quad z \leq \varepsilon. \end{aligned}$$

Here, $\boldsymbol{J}$ is the Jacobian of the QS vector, and $\boldsymbol{J}_{i:f_i(\boldsymbol{x})\geq r_i}$ denotes the rows of the Jacobian $\boldsymbol{J}$ indexed by $i : f_i(\boldsymbol{x}) \geq r_i$. ε is an arbitrary positive constant, and the solution vector $\boldsymbol{c}$ is normalized using any desirable metrics such as the l^2-norm. The first set of constraints correspond to the QS functions $f_i(\boldsymbol{x}) \geq r_i$, and these are the only QS functions that need to be convex in PALD. Thus, PALD provides better support for non-convex QS optimization as compared to MGDA. Moreover, randomly choosing different initial points can also help deal with non-convex QS functions in this sense.

7 What-if Model

Tempo's Optimizer depends on the What-if Model to predict the values of QS metrics for a given workload under a given RM configuration. The What-if Model breaks each prediction into two steps and leverages the Workload Generator and Schedule Predictor respectively for these steps. Note that the QS metric is expressed as a function of the task schedule of the workload under the given RM configuration. The Workload Generator is responsible for generating the workload, and the Schedule Predictor is responsible for generating the task schedule given the workload and the RM configuration.

7.1 Workload Generation

There are two ways to make workload information available to Tempo: replaying historical traces or using a statistical model of the workload (see Figure 3). The statistical model, which is usually trained from historical traces, has some key advantages. The model can be used to generate multiple synthetic workloads with the same distribution in order to test the sensitivity of parameter settings. More importantly, the model can be used to generate synthetic workloads with extended characeristics such as a growth in data size by 30%. For example, we developed a statistical model based on one month of historical traces from Company ABC's production database workload. The workload distributions from Company ABC (reported further in the evaluation section) are similar to the distributions described in [40]. In particular, the task duration approximately follows a lognormal distribution, and the job arrival approximately follows a Poisson process.

7.2 Fast Schedule Prediction

Given a workload generated as above, the Schedule Predictor in Figure 3 estimates the task schedule of the workload under a given RM configuration. Since the What-if Model needs to explore the impact of many different RM configurations, fast prediction of schedules can speed up Tempo's optimization process significantly.

For very fast task schedule simulation, we implemented a Schedule Predictor for the RMs used in Hadoop, Spark, and YARN using time warp mechanism [28]. Our implementation computes the cluster resource usage at only the submission time, tentative finish time, and possible preemption time of each task, based on the workload information and RM configuration parameter settings. This technique helps the Predictor get rid of actually running the tasks as well as synchronization within the RM.

To extend to other RMs, Tempo can leverage existing RM simulators that have already been developed for several popular systems, such as Borg [47], Apollo [10], Omega [41], MapReduce [46, 25, 24], and YARN [7]. Most of these existing simulators are designed to reproduce the real-time behavior of the RM, which is a superset of our goal of computing the task schedule efficiently.

8 Evaluation

The evaluation consists of two parts. The first part validates the components of Tempo based on real workload traces from the production database at Company ABC running on Hadoop. The second part does an end-to-end evaluation of Tempo using production workload traces from Company ABC, Facebook, and multiple customers of Cloudera [12]. We apply Tempo to four real-life scenarios and show, respectively, the improvements in job response time, resource utilization, adaptivity to workloads variations, and predictive resource provisioning. In the experiments where a baseline performance is needed for comparison, we used resource allocations as determined by expert DBAs and cluster operators in Company ABC. The following insights emerge from the evaluation:

- Tempo can tailor the resource allocation to SLO-driven business-critical workloads, and offers tenants the freedom to specify SLOs.
- Tempo improves the resource utilization by 15%, and job response time for best-effort tenants by 50% under 25% slack without breaking the deadlines for production workloads.
- Tempo effectively adapts to workload variations by periodically updating the RM configuration using a small window of most recent traces.
- Tempo can further help DBAs and cluster operators determine the appropriate cluster size for their multi-tenant parallel database for the given SLOs and workloads, minimizing the overall resource costs.

These results are due to: 1) informed resource allocation which takes into account the workload characteristics revealed from historical traces; and 2) optimized RM configurations aiming specifically for the SLOs because Tempo makes the connection between the RM configuration and SLOs more transparent and predictable.

8.1 Validating the schedule prediction

We begin by validating the task schedule prediction on a 700-node production cluster at Company ABC. In particular, we measure the accuracy of the prediction using one week's production workload from six independent tenants, as described in Table 2.1. The workload consist of approximately 60,000 jobs and 35 million production tasks collected in a noisy environment where there were job and task failures, jobs killed by users and DBAs, and node blacklisting and restarts. Figure 5 shows the key statistics of the workload.

The schedule prediction for the 35 million tasks from six tenants takes just 4 minutes, or approximately 150,000 tasks per second. We compare the predicted task schedule and the observed schedule based on the traces, and compute the prediction error. Both the relative absolute error (RAE) and the relative squared error (RSE) are used as the error metrics. The RAE and RSE of tenant i are defined respectively as

$$\mathrm{RAE}_i = \frac{\Sigma_j |p_{ij} - l_{ij}|}{\Sigma_j |l_{ij} - \mathbb{E}_j[l_{ij}]|}, \quad \mathrm{RSE}_i = \sqrt{\frac{\Sigma_j (p_{ij} - l_{ij})^2}{\Sigma_j (l_{ij} - \mathbb{E}_j[l_{ij}])^2}} \ .$$

Here p_{ij} and l_{ij} represent the predicted and observed finish time of job j for tenant i, respectively. Table 8.1 gives the RAE and RSE for the estimated job finish time. As can be seen, the highest error (24.4%) was incurred for the MV tenant in Company ABC. Most jobs from MV were long-running

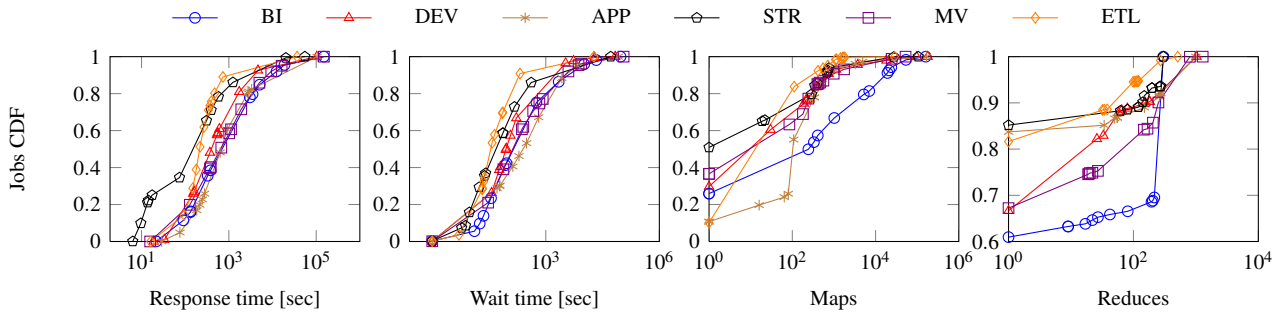

Figure 5: Key statistics of Company ABC's workloads.

Tenant	RAE	RSE	Tenant	RAE	RSE
BI	0.1585	0.2210	STR	0.1610	0.1463
DEV	0.2195	0.2267	MV	0.2318	0.2437
APP	0.1812	0.1599	ETL	0.1210	0.1908

Table 2: Job finish time estimation errors for each tenant.

jobs, especially with large duration of reduce tasks. We observed a considerable amount of killed reduce tasks for MV due to preemptions. For killed and failed tasks, the task start time and finish time are not recorded accurately in workload traces; which explains why MV has a higher prediction error than others.

8.2 End-to-end evaluation

The end-to-end experiments involve four real-life scenarios, and were performed on a 20-node Amazon EC2 cluster with m3.xlarge instances. The production workload traces from Company ABC, Facebook, and Cloudera customers were scaled and replayed on the EC2 cluster using SWIM [12]. In addition, the initial RM configuration was derived directly from the expert one created by DBAs for Company ABC's production database. As shown in the previous experiment, the schedule prediction for processes 150,000 tasks per second. Each end-to-end experiment involves approximately 30,000 tasks from two tenants, and each Tempo control loop explores 5 RM configuration candidates. Thus, one Tempo control loop requires prediction for roughly 150,000 tasks, which takes one second.

8.2.1 Mix of deadline-driven and best-effort workloads

The first scenario involves two tenants running workloads which come with the deadline SLO specified with QS_{DL}, and the low average job response time SLO specified with QS_{AJR}, respectively. The experiment aimed to obtain an RM configuration which is better than the expert one used in production. In particular, under the new RM configuration, *every* job from the deadline-driven workload must complete no later than the completion of the same job under the expert RM configuration. This is a strict constraint, where the deadlines in QS_{DL} are given by the completion times of deadline-driven jobs under the expert RM configuration, and the corresponding $r_i = 0$ (for 0% deadline violations). Another constraint involving QS_{AJR} enforces that the average job response time of the best-effort workloads under the new RM configuration cannot be greater than the average job response time (r_i) under the expert configuration.

When counting the number of deadline violations, a 25% slack, i.e., $\gamma = 0.25$, is used in QS_{DL} to reduce the sensitivity to noise, since the workloads under the same RM configuration with a slack 0 ($\gamma = 0$ in QS_{DL}) can yield a large deadline violation fraction (up to 83%).

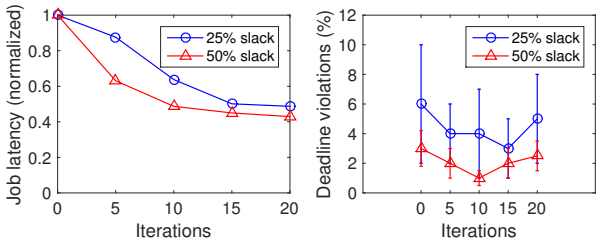

Figure 6: Average job response time for the best-effort tenant (left) and fraction of deadline violations for the deadline-driven tenant (right) at each iteration.

Figure 6 shows the SLOs (QS values) at each iteration in the Tempo control loop. At the iteration 0, the initial expert RM configuration was used. The RM configuration was then iteratively optimized by the Tempo control loop. It can be seen that, at convergence, the improvements in average job response time of the best-effort tenant are 50% and 58% for 25% and 50% slack, respectively. The gap between the improvements is relatively small, i.e., 8%. One reason is that both improvements benefited from the reduced contention for resources, which is confirmed in the next experiment. In addition, the fraction of deadline violations first drops and then breaks even at convergence. This trend is due to the fact that once the Pareto frontier is reached, we cannot improve one SLO without sacrificing another.

8.2.2 Improving resource utilization

In addition to the previous scenario, this experiment considered a third SLO, high resource utilization, which is specified

with QS_{UTIL}. We focused exclusively on MapReduce workloads due to the observation of significant task preemptions in production. The experiment added two constraints corresponding to the map container utilization and reduce container utilization, respectively. The r_i's were set according to the measured map and reduce container utilization under the expert RM configuration. The results show fewer preemptions under the Tempo optimized RM configuration as well as improvements in job response time subject to the deadline SLOs.

As we discussed, preemption happens when a tenant has been starved for a certain period of time (the configured preemption timeout), killing a certain number of most recently launched tasks from other tenants. Thus, preemption results in lost work and decreased resource utilization. Each tenant can specify a per-tenant preemption timeout in the RM configuration, and these settings are difficult to get right due to their complex connections to workloads and SLOs.

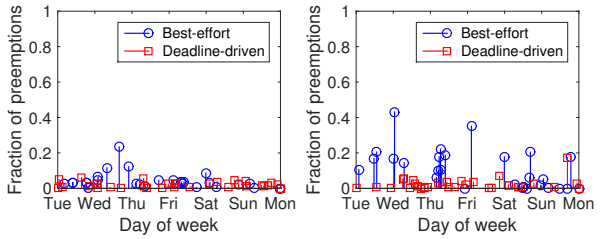

Figure 7: Task preemptions for MapReduce workloads at Company ABC. On the left shows the preempted map tasks, and the preempted reduce tasks are given on the right.

We observed a significant number of preempted MapReduce tasks on the production cluster at Company ABC. Figure 7 shows the map and reduce preemptions over the period of one week. During this period, 6% map tasks and 23% reduce tasks had been preempted, and the reduce preemptions were mostly from the best-effort tenant. The main reason was that the workloads of the best-effort tenant contain mostly long-running reduce tasks, as shown in Figure 8.

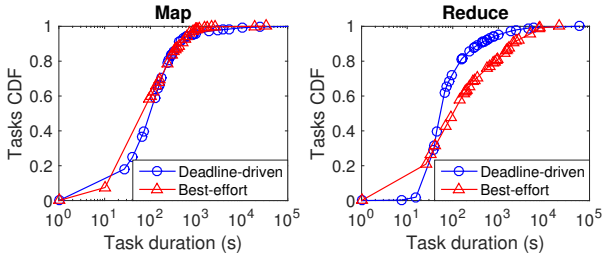

Figure 8: Task duration distributions for MapReduce workloads at Company ABC.

Figure 9 shows the SLOs under the original expert RM configuration and the Tempo optimized RM configuration. As can be seen, the optimized resource allocation delivers 22% improvement in the average job response time of the best-effort tenant workloads and 10% in the deadline QSs. Another improvement is in the utilization of reduce containers, while the utilization of map containers remains at the same level. The results are consistent with our observations of preemption statistics, and the improvements in reduce container utilization is due to the alleviated preemptions. In particular, the preemption timeout settings in the Tempo-optimized RM configuration had been self-tuned appropriately to the workload distribution.

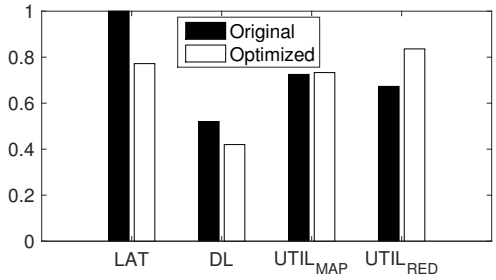

Figure 9: SLOs under the original and optimized (slack = 0) RM configuration: AJR, DL, $UTIL_{MAP}$, and $UTIL_{RED}$ are the average job response time of the best-effort tenant, fraction of deadline violations for the deadline-driven tenant, map container utilization, and reduce container utilization, respectively.

8.2.3 Adaptivity to workload variations

In this experiment, we applied Tempo to meet SLOs under slowly changing workload distributions. Figure 10 depicts the instant job response time distribution for deadline-driven and best-effort tenants. The instant job response time is computed using the moving average of a 30-min window. As can be seen, the instant job response time of deadline-driven workloads exhibits a periodic pattern while the job response time of the best-effort workloads changes dramatically over time.

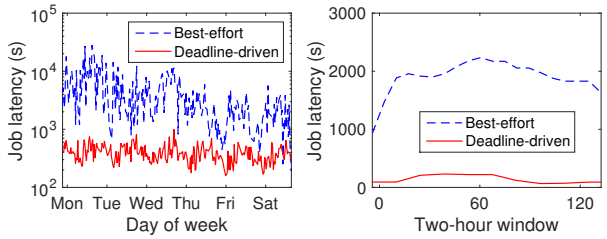

Figure 10: Instant job response time distributions. On the left shows the production workloads of Company ABC over the period of a week. On the right gives the two-hour experiment workloads on EC2 using Facebook and Cloudera traces.

Recall that each iteration of Tempo control loop uses a fixed-length interval of most recent job traces as input. The next experiment evaluates how different interval lengths impact Tempo's performance.

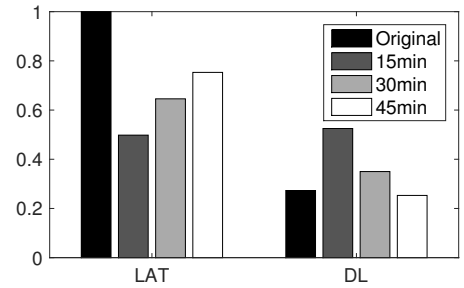

Figure 11: SLOs for different interval lengths in Tempo control loop. AJR denotes the normalized average job response time of the best-effort workloads, and DL represents the fraction of deadline violations (computed via QS_{DL} with slack $\gamma = 25\%$).

Figure 11 shows the SLOs under the original expert RM configuration and Tempo optimized RM configurations for interval length 15min, 30min, and 45min. Similarly, the experiment uses SLOs specified with QS_{AJR}, and QS_{DL} (25% slack). As can be seen, a small window size favors the average job response time of the best-effort workloads while leading to a higher percent of deadline violations. According to the results, the 45min interval length yields a similar fraction of deadline violations as the original RM configuration, but a 22% improvement in the average job response time of the best-effort workloads. The results show that Tempo can adapt to workload variations using a small interval length.

8.2.4 Resource provisioning and cutting costs

The last experiment demonstrates the application of Tempo to resource provisioning, estimating the minimum amount of resources needed to meet the given SLOs. This application can help users do better resource planning and cut overprovisioning costs. In addition, this application can bridge the gap in resource allocation between the development cluster and the production cluster, that is, converting the resource allocation on the development cluster for use in the production cluster.

The experiment involves running the same given deadline-driven workloads and best-effort workloads on three EC2 clusters with 20 nodes (100%), 10 nodes (50%), and 5 nodes (25%), respectively. Tempo was used to estimate the SLOs of the workloads when executed on the 100% cluster, using traces respectively from the 100% cluster, 50% cluster, and 25% cluster. This experiment mimics the scenario in which users collect traces of the workload on the current cluster, and would like to know how a new cluster size will impact the SLOs. (From our experience, this use case is common at companies like LinkedIn and Yahoo.) In this case, Tempo can serve as a key component in the decision-making for resource provisioning.

Figure 12 gives the SLO estimation errors using traces from equal and smaller clusters. As can be seen, Tempo can

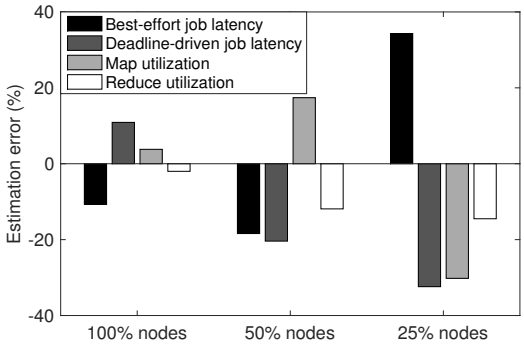

Figure 12: Errors in SLO estimation using traces based on equal and smaller cluster sizes.

predict—with the error no more than 20%—the SLOs of the current workloads run on a double-size cluster; using traces collected from the current cluster. Predicting the SLOs of the current workloads run on a quadruple-size cluster results in a maximum error of 35%.

9 Related Work

Most Resource Managers (RMs) that are deployed on multi-tenant "big data" database systems today like RedShift, Teradata, Vertica, Hadoop, and Spark are based on simple resource allocation principles such as static resource partitioning [1], *max-min fairness* [4, 3], or *dominant resource fairness* [22, 21, 42]. Quincy [27] is a Fair scheduler which takes into account data locality as a preference. Choosy [22] further extends the max-min fairness to support hard job placement constraints.

Parallel database systems like IBM DB2 PE, RedShift, Teradata, and Vertica have RMs (usually called Workload Managers) that allow DBAs to specify *filter*, *throttle*, and *workload* rules to dynamically adjust the resource allocation of tenants. For example, a filter rule can reject unwanted logon and query requests before they are executed; a throttle rule can restrict the number of requests simultaneously executed against a database object. In addition, some databases allow user-defined events relevant to workload management to be defined and actions taken based on them. RedShift and Vertica use resource pools where each pool has parameters such as resource limits, priorities, and maximum concurrency like the RM configuration described in Section 3.2.

Mesos [26] introduces two-level resource allocation to support other custom RMs and improves data locality while allocating resources to tasks. YARN [44] separates computation and resource management by introducing a resource layer. Corona [2] uses a dedicated job tracker for each job to improve cluster utilization, and adopts a push-based scheduling model to improve the scalability. Omega [41] improves the scalability of RMs using parallelism, shared state, and lock-free optimistic concurrency control. Sparrow [39] is a

stateless scheduler that aims for low job response time in task scheduling, leveraging load-balancing techniques. It supports multiple schedulers as well as job and task placement constraints. Fuxi [49] enhances the fault tolerance and scalability of RMs by introducing user-transparent failure recovery features and a failure detection mechanism. Apollo [10] is another shared-state scheduling framework, and takes into account the data locality and server load to achieve high-quality scheduling decisions. Apollo also introduces opportunistic scheduling to improve cluster utilization, and unexpected cluster dynamics by detecting abnormal runtime behaviors.

Unlike Tempo, all the above RMs leave it to DBAs and cluster operators to create specific resource allocation policies as plugins. Other RMs have been proposed recently that take certain tenant-level SLOs into consideration. Rayon [14] introduces reservation-based scheduling to make resource allocation more predictable by planning in advance. The planning also increases the resource utilization. Rayon considers two types of jobs, production and best-effort jobs, and seeks to meet the completion deadlines of the production jobs and reduce completion latency of the best-effort jobs. However, unlike our work, Rayon is 1) intrusive in that it makes changes that cannot be applied easily to a wide class of RMs in multi-tenant database systems; 2) supports only two types of SLOs; 3) can be potentially wasteful by reserving resources in the presence of job failures, and 4) may still need the user/DBA to determine how much resources need to be reserved to meet SLOs, which is difficult.

In [30], the authors develop a deadline estimation model and apply real-time scheduling to meet job deadlines. ARIA [45] provides support for job deadlines by profiling jobs and modeling resource requirements in order to complete before the deadline. WOHA [33] improves workflow deadline satisfactions in Hadoop. Tetris [23] avoids resource fragmentation by introducing multi-resource packing of tasks to machines. Tetris improves the average job completion time, and achieves high cluster makespan. The authors show that task packing can also work without significantly violating the fairness. Tetris lacks the rich support for SLOs that Tempo provides.

Pisces [42] focuses on datacenter-wide per-tenant performance isolation and fairness for multi-tenant cloud storage. Amoeba [8] delivers lightweight elasticity to compute clusters by splitting original tasks into smaller ones, and allowing safe exit of a running task and later resuming the task by spawning a new task for its remaining work. These features can help reduce the cost of preemption. Pulsar [9] is a resource management framework similar to Tempo. Pulsar provides end-to-end performance isolation through a *virtual datacenter abstraction (VDC)* which essentially encapsulates resource demand forecasting and QS metrics for each tenant. However, Pulsar focuses on sufficient resource scenarios and does not support multiple performance goals associated with each tenant as well as their trade-offs in a limited resource setting. The effectiveness of Pulsar also relies on the accuracy of user-specified cost functions in VDCs and resource demand estimation. Unlike Tempo, robust resistance to noise (inaccuracies in both cost and demand estimation) is not guaranteed in Pulsar.

Personalized Service Level Agreements (PLSAs) are introduced in [38] which serve as cost models connecting resources and SLOs. PLSAs can be used as QS metrics in Tempo based on SQL queries executed by each tenant.

We also briefly summarize main related work on the various classes of multi-objective optimization problems, and discuss their limitations with respect to what Tempo provides.

- **Convex and noiseless objective function:** This scenario can be solved using the well-known weighted sum scalarization. An alternative method, multiple gradient descent (MGDA), is proposed in [19] for solving the weighted sum scalarization problem. Another notable approach is Normal Boundary Intersection (NBI) [15], which allows evenly finding the Pareto frontier.
- **Non-convex and noiseless objective function:** One recent approach is conic scalarization (CS) [29], in which a new scalarization method is proposed to achieve Benson and Henig proper efficiency. However, the choice of the weight vector is not addressed in CS. There are also several evolutionary algorithms [17, 18, 31], which assume noiseless or low-noise situations, but are expensive to run.
- **Convex and noisy objective function:** In [35], the authors present a stochastic primal-dual algorithm for a single objective but multiple constraint problem; and it does not seek a Pareto-optimal solution. Noticeably, MGDA [19] could potentially be extended to the noisy scenario, but it does not handle the first set of constraints in the problem (SP1).
- **Non-convex and noisy objective function:** A prediction-based approach is proposed in [50]. This method estimates the Pareto frontier under the Gaussian assumption of the loss objectives, and does not specifically take into account the preference constraints.

10 Conclusion and Future Work

Meeting the SLOs of business-critical workloads while achieving high resource utilization in multi-tenant "big data" database systems is an important problem. The vast majority of resource allocators/schedulers deployed on multi-tenant database systems today rely on the DBAs to configure low-level resource settings. This process is brittle and increasingly hard as workloads evolve, data and cluster sizes change, and new workloads are added. In this paper, we presented a framework, Tempo, which enables DBAs to work with high-level SLOs conveniently. We demonstrated in both theory

and practice that Tempo is self-tuning and robust for achieving guaranteed SLOs in production database systems.

The current implementation of Tempo can simulate RMs like Mesos and YARN efficiently, using the time warp mechanism. Tempo can leverage RM simulators that have already been developed for several popular systems such as Borg, Apollo, and Omega. However, most of these simulators are designed to reproduce the real-time behavior of the RM, which may not deliver comparable efficiency as time warp simulation. Thus, one interesting direction is to add effective support for other RMs in Tempo.

The SLO abstraction in Tempo, i.e., QS metrics, allows each tenant to specify one or more SLOs, which apply to all workloads of the tenant. The effective spectrum of the SLOs corresponds to the structure of resource configurations in popular RMs like Mesos and YARN, where parameters are grouped by tenants (also known as pools or queues). To support more fine-grained SLOs among workloads of the same tenant, one workaround is to create hierarchical tenants as used in the Hadoop Capacity Scheduler. One future direction in Tempo is to provide native fined-grained SLO support for workloads from the same tenant.

A third direction is to explore scenarios where each tenant executes workloads exhibiting a mix of statistical characteristics. The current optimization in Tempo exploits the observation that workloads from the same tenant follow relatively fixed statistical characteristics. This assumption alleviates us from the restriction of having to observe historical executions of a newly-submitted job (both recurring and ad-hoc). To support workloads with a mix of statistical characteristics, one potential approach is to decompose the workloads and then distribute the workloads to separate tenants.

References

[1] Amazon redshift. `http://goo.gl/nS8cQH`.

[2] Facebook corona. `https://goo.gl/MN9VpK`.

[3] Hadoop capacity scheduler. `https://goo.gl/hh6Ood`.

[4] Hadoop fair scheduler. `https://goo.gl/8Ov2nj`.

[5] Teradata. `http://goo.gl/TjU7qR`.

[6] Vertica. `http://tinyurl.com/ovgufev`.

[7] Yarn scheduler load simulator. `https://goo.gl/JNUPoj`.

[8] ANANTHANARAYANAN, G., DOUGLAS, C., RAMAKRISHNAN, R., RAO, S., AND STOICA, I. True elasticity in multi-tenant data-intensive compute clusters. In *SOCC* (2012), pp. 24:1–24:7.

[9] ANGEL, S., BALLANI, H., KARAGIANNIS, T., O'SHEA, G., AND THERESKA, E. End-to-end performance isolation through virtual datacenters. In *OSDI* (2014), pp. 233–248.

[10] BOUTIN, E., EKANAYAKE, J., LIN, W., SHI, B., ZHOU, J., QIAN, Z., WU, M., AND ZHOU, L. Apollo: Scalable and coordinated scheduling for cloud-scale computing. In *OSDI* (Oct. 2014), pp. 285–300.

[11] BOYD, S., AND VANDENBERGHE, L. *Convex Optimization*. Cambridge University Press, 2004.

[12] CHEN, Y., ALSPAUGH, S., AND KATZ, R. Interactive analytical processing in big data systems: A cross-industry study of mapreduce workloads. *PVLDB 5*, 12 (Aug. 2012), 1802–1813.

[13] CLEVELAND, W. S., AND DEVLIN, S. J. Locally weighted regression: An approach to regression analysis by local fitting. *Journal of the American Statistical Association 83* (1988), 596–610.

[14] CURINO, C., DIFALLAH, D. E., DOUGLAS, C., KRISHNAN, S., RAMAKRISHNAN, R., AND RAO, S. Reservation-based scheduling: If you're late don't blame us! In *SOCC* (2014), pp. 2:1–2:14.

[15] DAS, I., AND DENNIS, J. E. Normal-boundary intersection: A new method for generating the pareto surface in nonlinear multicriteria optimization problems. *SIAM J. on Optimization 8*, 3 (Mar. 1998), 631–657.

[16] DAS, S., NARASAYYA, V., LI, F., AND SYAMALA, M. Cpu sharing techniques for performance isolation in multi-tenant relational database-as-a-service. vol. 7, p. 12.

[17] DEB, K., PRATAP, A., AGARWAL, S., AND MEYARIVAN, T. A fast and elitist multiobjective genetic algorithm: Nsga-ii. *Trans. Evol. Comp 6*, 2 (Apr. 2002), 182–197.

[18] DEB, K., SUNDAR, J., N, U. B. R., AND CHAUDHURI, S. Reference point based multi-objective optimization using evolutionary algorithms. In *International Journal of Computational Intelligence Research* (2006), pp. 635–642.

[19] DÉSIDÉRI, J.-A. Multiple-gradient descent algorithm (MGDA) for multiobjective optimization. *Comptes Rendus Mathématique Tome 350*, Fascicule 5-6 (Mar. 2012), 313–318.

[20] FERGUSON, A. D., BODIK, P., KANDULA, S., BOUTIN, E., AND FONSECA, R. Jockey: Guaranteed job latency in data parallel clusters. In *EuroSys* (2012), pp. 99–112.

[21] GHODSI, A., ZAHARIA, M., HINDMAN, B., KONWINSKI, A., SHENKER, S., AND STOICA, I. Dominant resource fairness: Fair allocation of multiple resource types. In *NSDI* (2011), pp. 323–336.

[22] GHODSI, A., ZAHARIA, M., SHENKER, S., AND STOICA, I. Choosy: Max-min fair sharing for datacenter jobs with constraints. In *EuroSys* (2013), pp. 365–378.

[23] GRANDL, R., ANANTHANARAYANAN, G., KANDULA, S., RAO, S., AND AKELLA, A. Multi-resource packing for cluster schedulers. *SIGCOMM 44*, 4 (Aug. 2014), 455–466.

[24] HAMMOUD, S., LI, M., LIU, Y., ALHAM, N. K., AND LIU, Z. MRSim: A discrete event based MapReduce simulator. 2993–2997.

[25] HERODOTOU, H., LIM, H., LUO, G., BORISOV, N., DONG, L., CETIN, F. B., AND BABU, S. Starfish: A self-tuning system for big data analytics. In *CIDR* (2011), pp. 261–272.

[26] HINDMAN, B., KONWINSKI, A., ZAHARIA, M., GHODSI, A., JOSEPH, A. D., KATZ, R., SHENKER, S., AND STOICA, I. Mesos: A platform for fine-grained resource sharing in the data center. In *NSDI* (2011), pp. 295–308.

[27] ISARD, M., PRABHAKARAN, V., CURREY, J., WIEDER, U., TALWAR, K., AND GOLDBERG, A. Quincy: Fair scheduling for distributed computing clusters. In *SOSP* (2009), pp. 261–276.

[28] JEFFERSON, D., SOWIZRAL, H., AND CORPORATION, R. *Fast Concurrent Simulation Using the Time Warp Mechanism: Part I, Local Control*. Fast Concurrent Simulation Using the Time Warp Mechanism: Part I, Local Control. Rand Corporation, 1982.

[29] KASIMBEYLI, R. A conic scalarization method in multi-objective optimization. *Journal of Global Optimization 56*, 2 (2013), 279–297.

[30] KC, K., AND ANYANWU, K. Scheduling hadoop jobs to meet deadlines. In *CLOUDCOM* (2010), pp. 388–392.

[31] KNOWLES, J. Parego: A hybrid algorithm with on-line landscape approximation for expensive multiobjective optimization problems. *Trans. Evol. Comp 10*, 1 (Sept. 2006), 50–66.

[32] LANG, W., SHANKAR, S., PATEL, J., AND KALHAN, A. Towards multi-tenant performance slos. In *ICDE* (2012).

[33] LI, S., HU, S., WANG, S., SU, L., ABDELZAHER, T., GUPTA, I., AND PACE, R. Woha: Deadline-aware map-reduce workflow scheduling framework over hadoop clusters. In *ICDCS* (2014), pp. 93–103.

[34] MACE, J., BODIK, P., FONSECA, R., AND MUSUVATHI, M. Retro: Targeted resource management in multi-tenant distributed systems. In *NSDI* (May 2015), pp. 589–603.

[35] MAHDAVI, M., YANG, T., AND JIN, R. Stochastic convex optimization with multiple objectives. In *NIPS*. 2013, pp. 1115–1123.

[36] NARASAYYA, V., DAS, S., SYAMALA, M., CHANDRAMOULI, B., AND CHAUDHURI, S. Sqlvm: Performance isolation in multi-tenant relational database-as-a-service. In *CIDR* (January 2013).

[37] NARASAYYA, V., DAS, S., SYAMALA, M., CHAUDHURI, S., LI, F., AND PARK, H. A demonstration of sqlvm: Performance isolation in multi-tenant relational database-as-a-service. In *SIGMOD* (2013), pp. 1077–1080.

[38] ORTIZ, J., DE ALMEIDA, V. T., AND BALAZINSKA, M. Changing the face of database cloud services with personalized service level agreements. In *CIDR* (2015).

[39] OUSTERHOUT, K., WENDELL, P., ZAHARIA, M., AND STOICA, I. Sparrow: Distributed, low latency scheduling. In *SOSP* (2013), pp. 69–84.

[40] REN, Z., XU, X., WAN, J., SHI, W., AND ZHOU, M. Workload characterization on a production hadoop cluster: A case study on taobao. In *IEEE International Symposium on Workload Characterization* (2012), pp. 3–13.

[41] SCHWARZKOPF, M., KONWINSKI, A., ABD-EL-MALEK, M., AND WILKES, J. Omega: Flexible, scalable schedulers for large compute clusters. In *EuroSys* (2013), pp. 351–364.

[42] SHUE, D., FREEDMAN, M. J., AND SHAIKH, A. Performance isolation and fairness for multi-tenant cloud storage. In *OSDI* (2012), pp. 349–362.

[43] TANG, S., LEE, B.-S., HE, B., AND LIU, H. Long-term resource fairness: Towards economic fairness on pay-as-you-use computing systems. In *ICS* (2014), pp. 251–260.

[44] VAVILAPALLI, V. K., MURTHY, A. C., DOUGLAS, C., AGARWAL, S., KONAR, M., EVANS, R., GRAVES, T., LOWE, J., SHAH, H., SETH, S., SAHA, B., CURINO, C., O'MALLEY, O., RADIA, S., REED, B., AND BALDESCHWIELER, E. Apache hadoop yarn: Yet another resource negotiator. In *SOCC* (2013), pp. 5:1–5:16.

[45] VERMA, A., CHERKASOVA, L., AND CAMPBELL, R. H. Aria: Automatic resource inference and allocation for mapreduce environments. In *ICAC* (2011), pp. 235–244.

[46] VERMA, A., CHERKASOVA, L., AND CAMPBELL, R. H. Play it again, simmr! In *CLUSTER* (2011), pp. 253–261.

[47] VERMA, A., PEDROSA, L., KORUPOLU, M. R., OPPENHEIMER, D., TUNE, E., AND WILKES, J. Large-scale cluster management at Google with Borg. In *EuroSys* (2015).

[48] XIONG, P., CHI, Y., ZHU, S., MOON, H. J., PU, C., AND HACIGUMUS, H. Intelligent management of virtualized resources for database systems in cloud environment. In *ICDE* (2011), pp. 87–98.

[49] ZHANG, Z., LI, C., TAO, Y., YANG, R., TANG, H., AND XU, J. Fuxi: A fault-tolerant resource management and job scheduling system at internet scale. *PVLDB 7*, 13 (Aug. 2014), 1393–1404.

[50] ZULUAGA, M., KRAUSE, A., SERGENT, G., AND PÜSCHEL, M. Active learning for multi-objective optimization. In *ICML* (2013).